Spurious oscillations and conservation errors in interface-capturing schemes

By E. Johnsen

1. Motivation and objectives

When shock-capturing schemes are applied to flows of multiple components, spurious oscillations usually develop at interfaces (e.g., in Mulder *et al.* 1992) and propagate through the flow, thus contaminating the solution. These perturbations are particularly problematic when small fluctuations are important flow features (e.g., in acoustics or turbulence), and in general multicomponent multi-dimensional flows where these errors may trigger undesirable instabilities at interfaces.

The present work focuses on interface-capturing schemes, in which interfaces are not resolved on the grid but are regularized over a few computational cells by adding numerical dissipation.† In the context of interface capturing, Abgrall (1996) traced such errors to the discontinuity in the ratio of specific heats in the energy equation and suggested a means to overcome this drawback for first- and second-order accurate quasi-conservative schemes. In the proposed quasi-conservative formulation, the Euler equations are still written in conservative form, so that correct shock speeds are achieved, but the transport equations used to describe the interface are non-conservative. Hence, the mass of each species is not exactly conserved. The correction proposed by Abgrall (1996) must be modified for higher-order accurate spatial discretizations, such as Weighted Essentially Non-Oscillatory (WENO) methods (Liu *et al.* 1994): Johnsen & Colonius (2006) showed that a reconstruction of the averaged primitive variables is required in a finite volume interface-capturing implementation of WENO to multicomponent flows. In relevant studies, Larrouturou (1991) observed that negative values of the mass fraction may be achieved.

The objective of the present paper is to assess the level at which conservation losses, spurious oscillations and negative mass fractions affect the solutions to multicomponent flow problems in an interface-capturing framework. Section 2 describes the governing equations and the numerical methods and Section 3 presents results for two test problems; in particular, the behavior of the error is studied for different formulations of the governing equations and under grid refinement. Finally, the findings are summarized and an outlook for future work is outlined.

2. Numerical methods

For simplicity, the 1-D Euler equations are considered:

$$\begin{pmatrix} \rho \\ \rho u \\ E \end{pmatrix}_t + \begin{pmatrix} \rho u \\ \rho u^2 + p \\ (E+p)u \end{pmatrix}_x = \mathbf{0}, \tag{2.1}$$

† In interface-tracking methods, such as the Ghost Fluid Method (Fedkiw *et al.* 1999) or pressure evolution algorithms (Karni 1994), oscillations are usually prevented by solving a different form of the equations at interfaces, so that errors in the conservation of total energy may occur.

where ρ is the density, u is the velocity, E is the total energy, p is the pressure, t denotes time and x denotes position. For ideal gases, the following equation of state closes the system:

$$E = \frac{p}{\gamma - 1} + \rho \frac{u^2}{2}, \tag{2.2}$$

where γ is the ratio of specific heats. When solving the system of Eqs. (2.1) and (2.2) for multiple fluids, an additional equation must be specified in order to determine the appropriate value of γ. In the present problems, the different fluid components are assumed immiscible. An interface between two fluid components can be represented by a discontinuity in γ. Since material interfaces are advected by the flow,

$$\phi_t + u\phi_x = 0, \tag{2.3}$$

where ϕ could be any function of the material properties, i.e., $\phi = \phi(\gamma)$. Thus, Eq. (2.3) specifies the location of the interface. Because Eq. (2.3) is not in conservative form, the system of equations is termed *quasi-conservative*. Using the continuity equation, the transport equation for material properties can be written in conservative form:

$$(\rho\phi)_t + (\rho u\phi)_x = 0. \tag{2.4}$$

In interface-capturing schemes, ϕ is usually a field variable. Numerical dissipation is introduced, such that interfaces diffuse over a few grid points, in analogy to shock capturing. Thus, even though the fluids are assumed immiscible, there exists a thin region between two fluids made up partly of one fluid, partly of another one. This *diffuse interface* is a purely numerical artifact and is expected to reduce to a sharp one as $\Delta x \to 0$. As a result, an appropriate definition of γ must be specified. Based on the definition of the mass fraction, $Y_i = \rho_i/\rho_m$, where the subscripts i and m denote one component and the mixture, respectively, and that of the gas constant, $R_m = R_u/M_m$, where R_u is the universal gas constant and M is the molar mass, the gas constant for a mixture of two components is given by:

$$\gamma_\mu = \frac{\gamma_1 Y_1 + \gamma_2 Y_2 \frac{M_1}{M_2}\frac{\gamma_1 - 1}{\gamma_2 - 1}}{Y_1 + Y_2 \frac{M_1}{M_2}\frac{\gamma_1 - 1}{\gamma_2 - 1}}, \tag{2.5}$$

with $Y_2 = 1 - Y_1$. Thus, ϕ could be a function of Y_1. Though desirable, a physical definition of γ within this diffuse region (i.e., using Eq. (2.5)) is not strictly required, since this region vanishes as the grid is sufficiently refined. In fact, in order to prevent spurious interface oscillations in first- and second-order accurate schemes, Abgrall (1996) uses the function,

$$\phi = \frac{1}{\gamma - 1} \quad \Rightarrow \quad \gamma = 1 + \frac{1}{\phi}, \tag{2.6}$$

to define γ directly in Eq. (2.2). Other functions of γ lead to interface oscillations (Karni 1994). A drawback of Eq. (2.6) is that additional equations must be added if the evolution of different gases of the same γ is considered. As an alternative, Shyue (1998) uses the mass fraction and defines

$$\phi = Y_1, \quad \text{with } \frac{1}{\gamma - 1} = \frac{Y_1}{\gamma_1 - 1} + \frac{1 - Y_1}{\gamma_2 - 1}. \tag{2.7}$$

Since $C_v = R/(\gamma - 1)$, Eq. 2.7 implies that the following assumption is made: $R_m = R_1 = R_2$, or, alternately, $M_m = M_1 = M_2$. R_m is not required to solve the multicomponent Euler equations supplemented by a transport equation for which γ is expressed

by Eq. (2.6) or Eq. (2.7), but is needed only in the post-processing of the results, e.g., if the temperature is of interest. On the other hand, if Eq. (2.5) is used, R_m must be initially specified in each fluid. In the formulations of Abgrall and Shyue, an initial distribution of $1/(\gamma-1)$ or Y_1 is specified and evolved according to the advection Eq. (2.3), with appropriate modifications to the Riemann solver. Thus, the equation of state varies smoothly across the interface.

A finite volume discretization of the equations of motion is currently employed. The governing equations can be written in semi-discrete form:

$$\frac{d\mathbf{q}}{dt}\Big|_i = -\frac{\mathbf{f}_{i+1/2} - \mathbf{f}_{i-1/2}}{\Delta x}, \tag{2.8}$$

where $\mathbf{q}$ is the vector of conserved variables and $\mathbf{f}_{i+1/2}$ is the numerical flux vector. A third-order accurate Total Variation Diminishing Runge-Kutta scheme is used for time marching (Gottlieb & Shu 1998). The spatial reconstruction is carried out in physical space† and is based on WENO (fifth-order accurate, unless otherwise mentioned); the Lax-Friedrichs (LF) solver is used for upwinding.

A difficulty with the non-conservative form of the transport Eq. (2.3) is that the approximate Riemann solvers must be modified accordingly (Saurel & Abgrall 1999). For instance, the semi-discrete version of Eq. (2.3) using LF is:

$$\frac{d\phi}{dt}\Big|_i = -\frac{\left[u_i \frac{\phi^R_{i+1/2}+\phi^L_{i+1/2}}{2} - \frac{\alpha(\phi^R_{i+1/2}-\phi^L_{i+1/2})}{2}\right] - \left[u_i \frac{\phi^R_{i-1/2}+\phi^L_{i-1/2}}{2} - \frac{\alpha(\phi^R_{i-1/2}-\phi^L_{i-1/2})}{2}\right]}{\Delta x}, \tag{2.9}$$

where the superscripts L and R denote the value of the function on the left and on the right of a cell edge, and α is the largest absolute value of the eigenvalue over the domain.

Several types of errors are highlighted in the following section. The first is the generation of spurious pressure oscillations due to the discontinuity in γ in the energy equation (Abgrall 1996). This error propagates to the momentum through the pressure gradient and thus alters the velocity, which in turn affects the density. A second error is the occurrence of mass fraction values outside of the allowed bounds because of an inconsistent coupling of the additional transport equation to the Euler system (Larrouturou 1991; Abgrall & Karni 2001). Finally, the third error considered in the present work pertains to the mass conservation of each species. The behavior of each of these errors depends on the system of equations that is solved. Table 2 summarizes the different formulations. Y stands for mass fraction, γ stands for the transport variable based on the ratio of specific heats, FC stands for fully conservative, QC for quasi-conservative (QCC implies that the conservative variables are reconstructed in the Euler equations, while QCP implies that the average primitive variables are reconstructed), M denotes the physical expression for γ, i.e., Eq. (2.5). The WENO variables refer to the variables that are reconstructed using the WENO procedure.

3. Results

In order to understand fundamental problems in interface-capturing schemes, two 1-D problems are considered: the advection of a material interface, which is studied in great detail, and the interaction of a shock with an interface, which is of practical relevance.

† A reconstruction in characteristic space may lead to smaller oscillations at interfaces, but will not remove them.

TABLE 1. Different schemes considered in the present study.

Scheme	Transport variable	Advection equation	Equation for γ	WENO variables
Y-FC-M	ρY_1	Eq. (2.4)	Eq. (2.5)	Conservative
Y-FC	ρY_1	Eq. (2.4)	Eq. (2.7)	Conservative
Y-QCC	Y_1	Eq. (2.3)	Eq. (2.7)	Conservative
Y-QCP	Y_1	Eq. (2.3)	Eq. (2.7)	Primitive
Y-QCP-M	Y_1	Eq. (2.3)	Eq. 2.5	Primitive
γ-QCP	$1/(\gamma-1)$	Eq. (2.3)	Eq. (2.6)	Primitive

3.1. *Advection of a material interface*

The simplest possible case of the advection of a material interface between two different gases is first studied in detail. A top-hat distribution of helium in nitrogen is moving at a constant velocity (equal to the sound speed in helium) with uniform pressure. The domain is periodic and has 101 points (unless otherwise mentioned), with grid spacing, $\Delta x = 0.02$. The variables are non-dimensionalized by the density, ρ_{He}, and sound speed, c_{He}, of helium, and the domain length, L. A constant $\Delta t/\Delta x = 0.4$ is used and the final time is $t_f c_{He}/L = 4.0$ (i.e., the solution is plotted after the interface has traveled two periods). The initial conditions are as follows:

$$\begin{aligned} \rho/\rho_{He} &= \frac{p_a/RT_a}{p_a/R_{He}T_a}, \\ \mathbf{u}/c_{He} &= (1,0,0), \\ p/\rho_{He}c_{He}^2 &= 1/\gamma_{He}, \\ Y_{He} &= \begin{cases} 1, & \text{if } -0.5 \le x \le 0.5, \\ 0, & \text{otherwise,} \end{cases} \end{aligned} \tag{3.1}$$

where the subscript a refers to ambient conditions and $Y_N = 1 - Y_{He}$.

First, the overall behavior of a fully conservative (Y-FC), and a quasi-conservative (Y-QCP) scheme, both of which employ the mass fraction as the relevant variable in the relevant transport equation. In the quasi-conservative scheme, the average primitive variables are reconstructed. Figure 1 shows profiles at t_f for both schemes. Oscillations are observed in all fields for the fully conservative scheme, particularly in the pressure and velocity; the density and γ achieve values outside of the allowed bounds. Somewhat surprisingly, the γ profile is more diffuse than in the quasi-conservative case. Because of the discontinuity in γ (Abgrall 1996) and because of the inconsistent coupling between the energy and transport equations (Johnsen & Colonius 2006),† the fully conservative scheme leads to an error in pressure at the end of the first time step. Due to the coupling of the energy, momentum and continuity equations, the pressure oscillations generate errors in the velocity and density fields as well. No oscillations are visible in the quasi-

† As shown in Johnsen & Colonius (2006), the advection form of the transport equation alone is not sufficient to prevent spurious interface oscillations for WENO schemes. If the traditional reconstruction of the conservative variables is carried out (Y-QCC scheme), oscillations are generated.

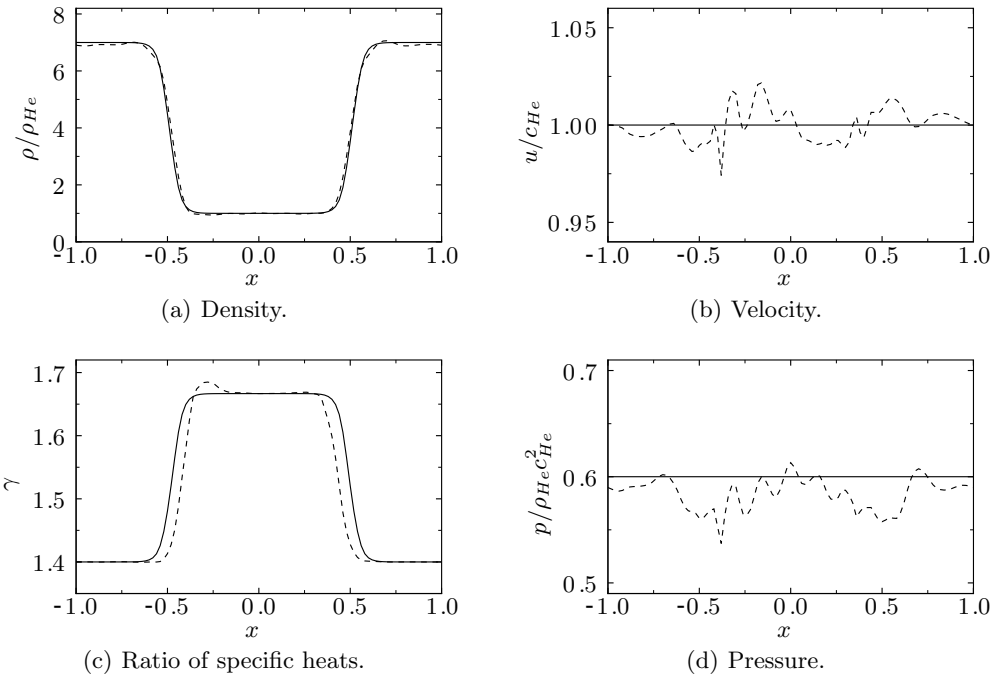

(a) Density. (b) Velocity.

(c) Ratio of specific heats. (d) Pressure.

FIGURE 1. Profiles at t_f for the advection of a distribution of helium in nitrogen. Dashed: fully conservative (Y-FC); solid: quasi-conservative (Y-QCP).

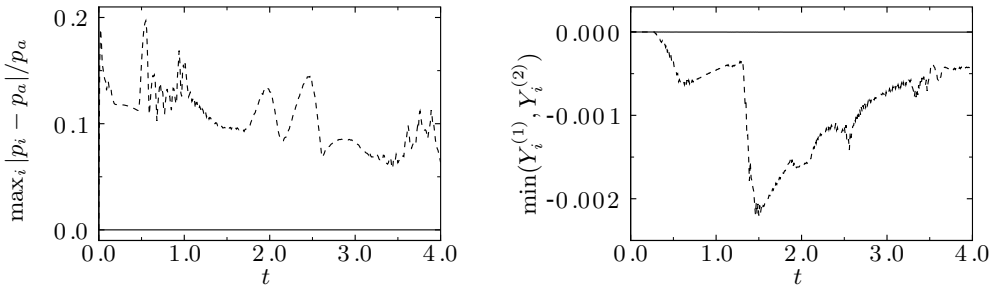

(a) Normalized L_∞ error in pressure. (b) Minimum mass fraction undershoot.

FIGURE 2. Advection of a top-hat distribution of helium in nitrogen. Dashed: fully conservative (Y-FC); solid: quasi-conservative (Y-QCP).

conservative scheme; in fact the only error in the pressure and velocity are at the round-off level (Johnsen & Colonius 2006).

Next, the pressure oscillations and undershoots in the mass fraction are quantified. Figure 2 shows the normalized L_∞ error in pressure and the minimum value of the mass fraction at every time step as a function of time. When using the fully conservative formulation (Y-FC), the pressure error can be large over the course of the simulation (up to 20%). In addition, the mass fraction may take a negative value, though the error is small (up to 2%); though not shown here, the upper bound is also overshot (i.e., $Y > 1$). This error in the mass fraction is important, because it affects the value of γ in the Euler

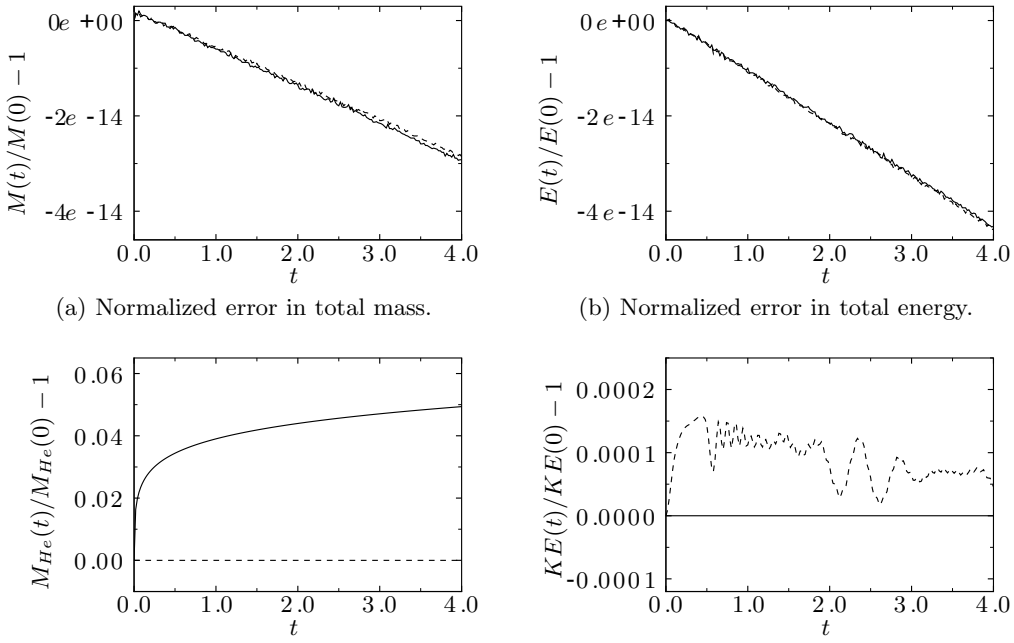

(a) Normalized error in total mass.

(b) Normalized error in total energy.

(c) Normalized error in mass of helium.

(d) Normalized error in kinetic energy.

FIGURE 3. Advection of a distribution of helium in nitrogen. Dashed: fully conservative (Y-FC); solid: quasi-conservative (Y-QCP).

equations. It should be noted that negative mass fractions are even observed in single-fluid problems (Abgrall & Karni 2001), in which case they do not affect the flow. On the other hand, the quasi-conservative scheme (Y-QCP) does not exhibit such problems, as the error is observed at the round-off level.

Next, the conservation errors are quantified. Figure 3 plots the normalized error in total mass, total energy, mass of helium, and total kinetic energy as a function of time. As expected from the conservative form of the Euler equations, the total mass and energy are conserved to the round-off level with both schemes. However, when using the quasi-conservative scheme (Y-QCP), the mass of helium increases over the course of the simulation, due to numerical dissipation; though not shown here, the mass of nitrogen follows a similar behavior, but decreases by mass conservation. The kinetic energy exhibits small oscillations in the fully conservative scheme (Y-FC) due to the fluctuating velocity field induced by the pressure oscillations.

In order to assess the effect of conservation errors and pressure oscillations, their dependence on the grid size is considered. Figure 4 shows the normalized L_∞ error in pressure and the minimum mass fraction for the fully conservative scheme (Y-FC), and the error in the mass of helium for the quasi-conservative scheme (Y-QCP) as a function of time for $N = 50$, 100, 200 and 400. When using the fully conservative scheme (Y-FC), the amplitude of the pressure oscillations decreases slightly with additional grid points; it is not clear whether the oscillations vanish or whether they converge to some value. When considering the quasi-conservative scheme (Y-QCP), the error in the total mass clearly decreases with additional grid points.

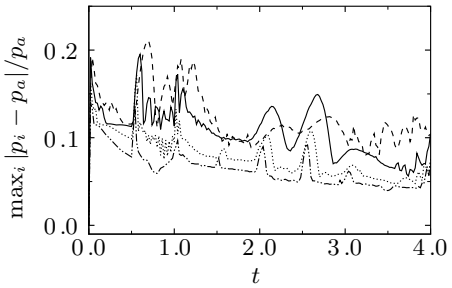

(a) Normalized L_∞ error in pressure (fully conservative scheme: Y-FC).

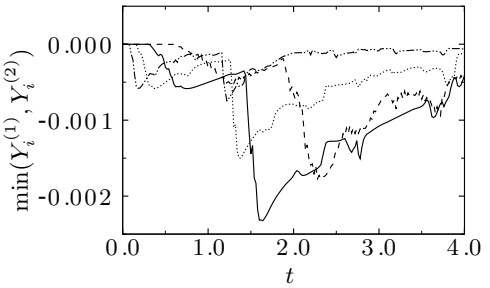

(b) Minimum mass fraction undershoot (fully conservative scheme: Y-FC).

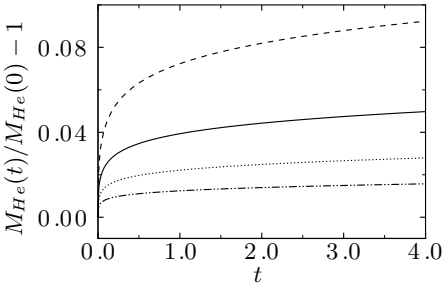

(c) Error in the mass of helium (quasi-conservative scheme: Y-QCP).

FIGURE 4. Advection of a distribution of helium in nitrogen. Dashed: $N = 50$; solid: $N = 100$; dotted: $N = 200$; dashed-dotted: $N = 400$.

The pressure oscillations and conservation errors are expected to be affected by the amount of dissipation of the scheme. This property is tested by considering different orders of accuracy of the WENO scheme. Figure 5 shows the normalized L_∞ error in pressure and the minimum mass fraction for the fully conservative scheme (Y-FC), and the total mass of helium for the quasi-conservative scheme (Y-QCP) as a function of time for different orders of accuracy of WENO. When using the fully conservative scheme, the pressure oscillations and undershoots in the mass fraction have similar amplitude but a higher frequency as the order of accuracy is increased. In the very dissipative first-order scheme, so much dissipation has been introduced that the mass fraction no longer achieves a value of zero after a given time. When using the quasi-conservative scheme (QCP), the error in the total mass of helium decreases as the order of accuracy is increased. This behavior is expected because a higher-order accurate reconstruction implies less dissipation.

Next, the difference between mass fraction-based (Y-QCP) and γ-based (γ-QCP) algorithms is considered. Figure 6 shows the γ profile at the end of the run and the error in mass of helium as a function of time. The γ profiles are virtually identical, thus implying little difference in the calculations of the Euler equations. However, the γ-based method shows slightly less dissipation in that a smaller mass of helium is lost.

Finally, the effect of the definition of γ is considered. Figure 7 shows the normalized L_∞ error in pressure, the minimum value of the mass fraction and the error in mass of helium as a function of time for the different definitions of γ based on Eqs. (2.5) and (2.7). Pressure oscillations are generated for the fully conservative schemes and when the

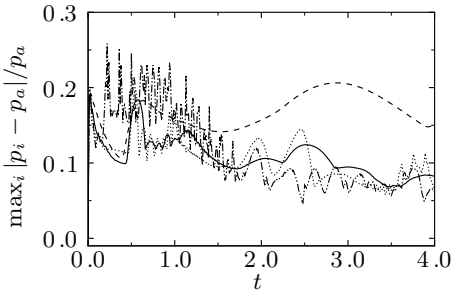

(a) Normalized L_∞ error in pressure (fully conservative scheme: Y-FC).

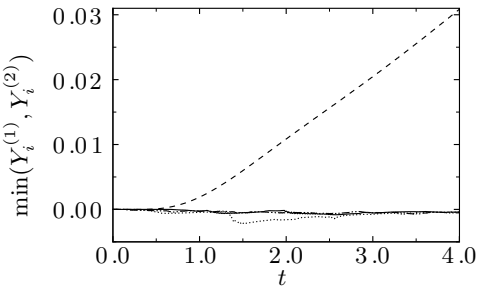

(b) Minimum mass fraction undershoot (fully conservative scheme: Y-FC).

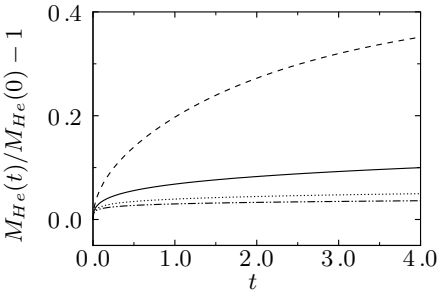

(c) Error in the mass of helium (quasi-conservative scheme: Y-QCP).

FIGURE 5. Advection of a distribution of helium in nitrogen. Dashed: WENO1; solid: WENO3; dotted: WENO5; dashed-dotted: WENO7.

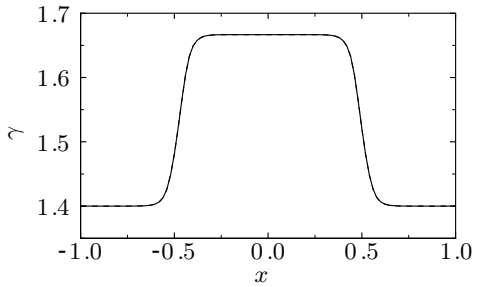

(a) Specific heat of helium at t_f.

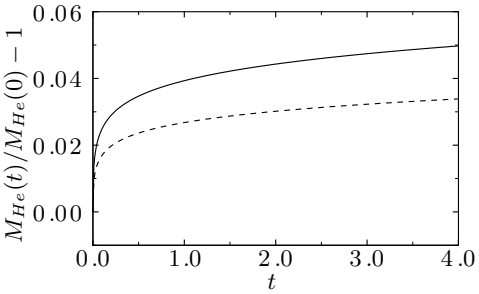

(b) Mass helium as a function of time.

FIGURE 6. Advection of a distribution of helium in nitrogen with quasi-conservative schemes. Dashed: γ; solid: mass fraction.

physical mixture definition is used (even in quasi-conservative form), while the quasi-conservative scheme with γ defined in Eq. (2.7) is the only scheme that does not generate pressure oscillations. Surprisingly, the fully conservative scheme with the physical mixture definition (Y-FC-M) shows smaller oscillations than the quasi-conservative scheme with the physical mixture definition (Y-QCP-M). For the mass fraction, the fully conservative scheme (Y-FC) leads to the largest errors, but this error decreases when the physical mixture definition is used. The quasi-conservative schemes hardly show any error on this scale. As expected, the fully conservative schemes lead to no errors in the mass of

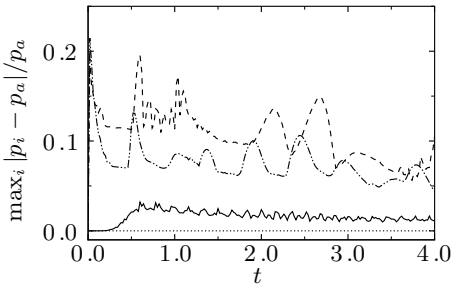

(a) Normalized L_∞ error in pressure.

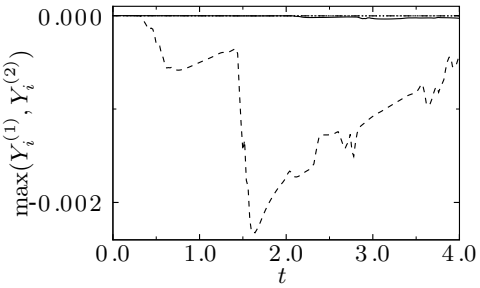

(b) Minimum mass fraction undershoot.

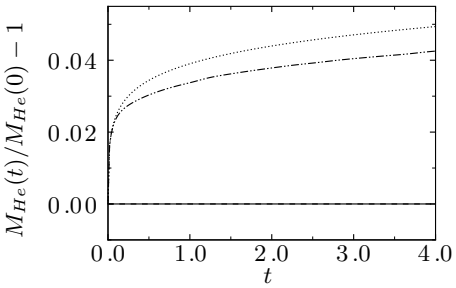

(c) Error in the mass of helium.

FIGURE 7. Advection of a distribution of helium in nitrogen. Dashed: fully conservative (Y-FC); solid: fully conservative with mixture (Y-FC-M); dotted: quasi-conservative (Y-QCP); dashed–dotted: quasi-conservative with mixture (Y-QCP-M).

helium, while the quasi-conservative schemes show a discrepancy; the scheme based on the physical definition of γ shows slightly less dissipation.

3.2. *Shock-interface interaction*

The most stringent 1-D test case is the interaction between a strong shock and an interface, as considered by Liu *et al.* (2003). A Mach 9 shock propagating in helium hits a nitrogen interface. The domain has 201 points, with grid spacing $\Delta x = 0.01$; non-reflecting boundary conditions are used. The variables are non-dimensionalized by the density and sound speed of helium, and the domain length, L. A constant CFL of $\Delta t/\Delta x = 0.05$ is used and the final time is $t_f c_{He}/L = 0.2$. The initial conditions are as follows:

$$
\begin{aligned}
\frac{\rho}{\rho_{He}} &= \begin{cases} \frac{(\gamma_{He}+1)M_s^2}{(\gamma_{He}-1)M_s^2+2}, & -1 \le x < -0.8, \\ \frac{p_a/RT_a}{p_a/R_{He}T_a}, & -0.8 \le x \le 1, \end{cases} \\
\frac{u}{c_{He}} &= \begin{cases} (-0.5) + \frac{2}{\gamma_{He}+1}\left(\frac{M_s^2-1}{M_s}\right), & -1 \le x < -0.8, \\ -0.5, & -0.8 \le x \le 1, \end{cases} \\
\frac{p}{\rho_{He}c_{He}^2} &= \begin{cases} \frac{p_a}{\rho_{He}c_{He}^2}\left[1 + \frac{2\gamma_{He}}{\gamma_{He}+1}(M_s^2-1)\right], & -1 \le x < -0.8, \\ \frac{p_a}{\rho_{He}c_{He}^2}, & -0.8 \le x \le 1, \end{cases} \\
Y_{He} &= \begin{cases} 1, & -1 \le x < -0.2, \\ 0, & -0.2 \le x \le 1, \end{cases}
\end{aligned}
\tag{3.2}
$$

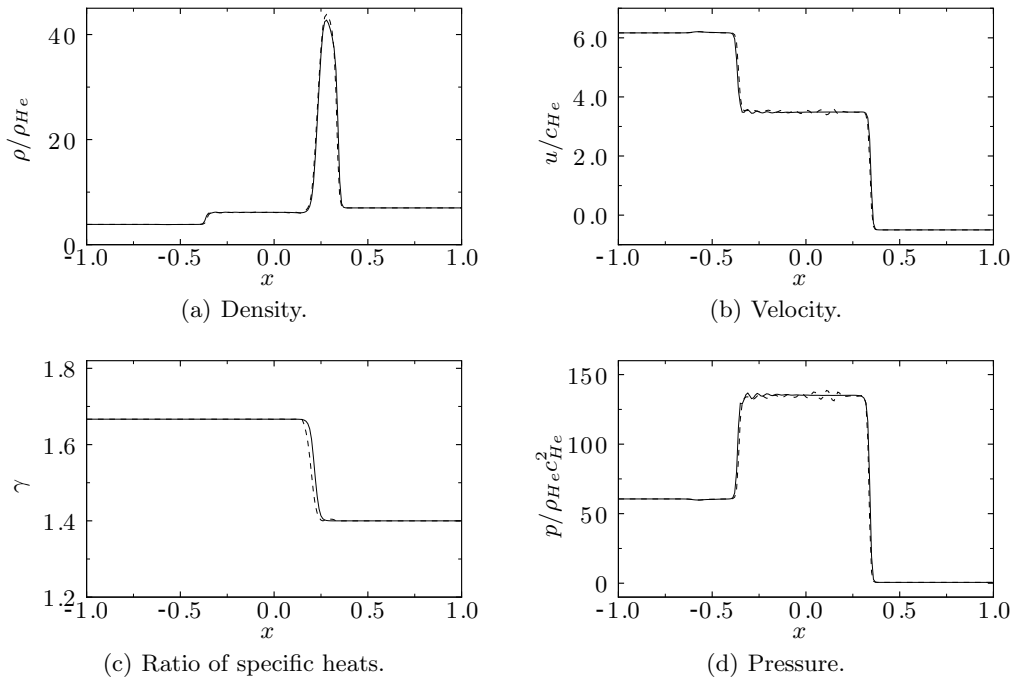

(a) Density. (b) Velocity.

(c) Ratio of specific heats. (d) Pressure.

FIGURE 8. Profiles at t_f for the shock-interface problem. Dashed: fully conservative scheme (Y-FC); solid: quasi-conservative scheme (Y-QCP).

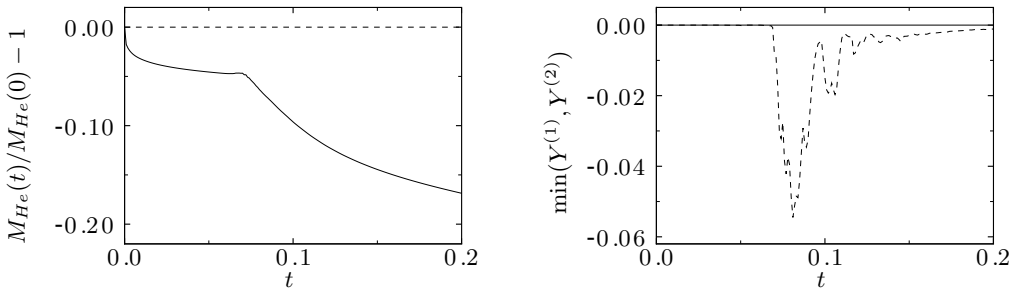

(a) Normalized mass of helium. (b) Minimum mass fraction undershoot.

FIGURE 9. Shock-interface interaction. Dashed: fully conservative scheme (Y-FC); solid: quasi-conservative scheme (Y-QCP).

where $Y_N = 1 - Y_{He}$, $R = R_u/M$ and $M_s = 9$. Clearly, the problem could have been studied as a Riemann problem starting at the time when the shock and interface coincide, but the present problem is more relevant to practical applications.

Figure 8 shows the density, velocity, γ and pressure profiles for the fully conservative (Y-FC) and quasi-conservative (Y-QCP) schemes using the mass fraction formulation. The solution corresponds that of a Riemann problem with a left-moving shock, and a right-moving material interface and shock. Oscillations are observed in the velocity and in the pressure with the fully conservative scheme. Because such large pressures are achieved, even small oscillations are large compared to other flow features. The location

of the material interface is slightly different; however the locations converge as the grid is refined. It should be noted that post-shock oscillations (Roberts 1990) are observed downstream of the left-moving shock, because of its slow speed relative to the grid.

Figure 9 shows the error in the mass of helium† and the minimum value of the mass fraction as a function of time. As expected, the quasi-conservative scheme exhibits an error in the mass of the left gas, due to the non-conservative form of the transport equation. The abrupt change in the slope occurs just as the shock hits the interface, thus highlighting the fact that this conservation error may depend on the velocity of the interface. The fully conservative scheme shows a large undershoot in the mass fraction (over 5%).

4. Conclusions and future work

In the present paper, the errors generated by different formulations of the governing equations for interface-capturing methods have been characterized. The problem of the advection of a material was investigated in detail, in order to understand the dependence of the errors on various properties; the interaction between a shock and an interface illustrated the effects of such errors in flows of practical interest. On one hand, spurious pressure oscillations, which then affect the momentum and density, and negative values of the mass fraction are observed when using a fully conservative scheme. The amplitude of the oscillations does not seem to decrease rapidly with grid refinement and the wavelength decreases with the order of accuracy of the scheme. On the other hand, quasi-conservative schemes do not conserve the mass of each species; though this error increases with time, it decreases as the grid is refined.

The long-term interest for the current work lies in multi-material mixing in Rayleigh-Taylor and Richtmyer-Meshkov instability. Therefore, it is absolutely necessary to have a basic understanding of the errors generated by the treatment of interfaces in compressible flows in order to correct such effects when more complex flows are considered. In order to run reasonable multi-dimensional problems, these schemes must be implemented in finite difference form, because of the cost of approximating the integral of the flux in the transverse direction. However, additional modifications are required for the quasi-conservative scheme in order to prevent the generation of spurious oscillations at interfaces.

Acknowledgements

The author is grateful for interesting discussions with Dr. Soshi Kawai and for the comments by Dr. Mehdi Raessi on the manuscript.

REFERENCES

Abgrall, R. 1996 How to prevent pressure oscillations in multicomponent flow calculations: a quasi conservative approach. *J. Comp. Phys.* **125** (1), 150–160.

Abgrall, R., & Karni, S. 2001 Computations of compressible multifluids. *J. Comp. Phys.* **169** (2), 594–623.

Fedkiw, R. P., Aslam, T., Merriman, B., & Osher, S. 1999 A non-oscillatory Eulerian approach to interfaces in multimaterial flows (the Ghost Fluid Method). *J. Comp. Phys.* **152** (2), 457–492.

† The mass of helium entering the domain from the left is subtracted.

Gottlieb, S., & Shu, C. W. 1998 Total variation diminishing Runge-Kutta schemes. *Math. Comp.* **67**, 73–85.

Johnsen, E. & Colonius, T. 2006 Implementation of WENO schemes in compressible multicomponent flows. *J. Comp. Phys.* **219** (2), 715–732.

Karni, S. 1994 Multicomponent flow calculations by a consistent primitive algorithm. *J. Comp. Phys.* **112** (1), 31–43.

Larrouturou, B. 1994 How to preserve the mass fractions positivity when computing compressible multi-component flows. *J. Comp. Phys.* **95** (1), 59–84.

Liu, X. D., Osher, S., & Chan, T. 1994 Weighted essentially non-oscillatory schemes. *J. Comp. Phys.* **115** (1), 200–212.

Liu, T. G., Khoo, B. C., & Yeo, K. S. 2003 Ghost fluid method for strong shock impacting on material interface. *J. Comp. Phys.* **190** (2), 651–681.

Mulder, W., Osher, S., & Sethian, J. A. 1992 Computing interface motion in compressible gas dynamics. *J. Comp. Phys.* **100** (2), 209–228.

Roberts, T. W. 1990 The behavior of flux difference splitting schemes near slowly moving shock waves. *J. Comput. Phys.* **90** (1), 141–160.

Saurel, R. 1999 A simple method for compressible multifluid flows. *SIAM J. Comput. Phys.* **21** (2), 1115–1145.

Shyue, K. M. 1998 An efficient shock-capturing algorithm for compressible multicomponent problems. *J. Comp. Phys.* **142** (1), 208–242.

Toro, E., Spruce, M., & Speares, W. 1994 Restoration of the contact surface in the HLL-Riemann solver. *Shock Waves* **4** (1), 25–34.